Rapid Communications

Production of Over-Dense Plasmas by Launching of 2.45 GHz Electron Cyclotron Waves on the Compact Helical System

IKEDA Ryosuke, TAKEUCHI Masaki, ITO Takafumi, TOI Kazuo[1)], SUZUKI Chihiro[1)],
MATSUNAGA Go[2)], SHOJI Tatsuo, MATSUOKA Keisuke[1)],
OKAMURA Shoichi[1)] and CHS Exp. Group[1)]

Department of Energy and Engineering Science, Nagoya University, Nagoya 464-8603, Japan
[1)]National Institute for Fusion Science, Toki 509-5292, Japan
[2)]Japan Atomic Energy Research Institute, Naka 311-0193, Japan

(Receive 20 July 2004 / Accepted 20 May 2005)

A simulation experiment of high temperature plasma transport using low temperature plasma having dimensionless parameters similar to those of a high temperature plasma is currently underway in the Compact Helical System. To produce such a plasma, 2.45 GHz microwaves up to 20 kW were injected perpendicularly to the toroidal field at B_t < 0.1 T. In the case at B_t = 0.0613 T, the maximum electron density reached three times that of the O-mode cutoff density. The measured power deposition was localized in the plasma core region beyond the Left-hand cutoff layer. These results clearly suggest that the over-dense plasma was produced and heated by electron Bernstein waves converted from launched X-mode in the peripheral region with a steep density gradient.

Keywords

helical device, over-dense plasma, electron cyclotron wave, electron Bernstein wave

A new transport simulation based on the concept "dimensional similarity" using a low temperature and density helical plasma is currently underway in the Compact Helical System (CHS), where it has the same dimensionless plasma parameters except the normalized ion gyro-radius [1,2]. Here, we attempted to generate this low temperature and density plasma at very low toroidal field (B_t) with 2.45 GHz microwaves. Efficient plasma heating close to or above the O-mode (O-) cutoff density is required to test the above-mentioned new experimental approach over a wide parameter range.

Plasma production and heating using 2.45 GHz microwaves up to 20 kW is carried out in CHS, at B_t < 0.1 T. Electron density and temperature are measured by a triple Langmuire probe, and the density is calibrated by the line averaged electron density measured by a 2 mm microwave interferometer.

The microwaves are launched into a torus through a circular cross-section port in the outer board near the equatorial plane of the horizontally elongated section. The directivity of the incident wave will be fairly poor because the port diameter is comparable to the vacuum wavelength of the wave. Moreover, the polarizations of the electron cyclotron waves (ECWs) may not be well specified.

The contour plots of the magnetic field strength in the vertically and horizontally-elongated section of CHS are shown in Fig. 1, where the magnetic axis position is R_{ax} = 97.4 cm and B_t = 0.0613 T at $R = R_{ax}$. Under this condition, the fundamental and second harmonic electron cyclotron resonance (ECR) layers are placed near the last closed flux surface (LCFS) (ρ ~ 0.9; ρ is the normalized minor radius) in the vertically elongated section and at ρ ~ 0.7 in the horizontally elongated one, respectively. A typical waveform of the microwave-produced plasma is shown in Figs. 2(a) and 2(b). The line averaged electron density (n_e^{2mm}) is more than twice the O-cutoff density ($n_{c,o}$ = 7.4 × 10^{16} m^{-3}). Figures 2(c) and 2(d) show the contour of electron density (n_e) and temperature (T_e) on the plane of time and ρ. In the initial phase of discharge, the electron density profile is hollow, and

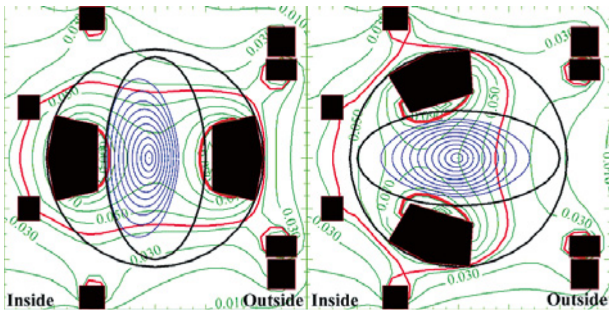

Fig. 1 Contours of the magnetic field strength and magnetic surfaces of CHS plasma at B_t = 0.0613 T and R_{ax} = 97.4 cm. The thick and thin red curves indicate the fundamental ECR and 2nd harmonic layers respectively.

author's e-mail: r.ikeda@nifs.ac.jp

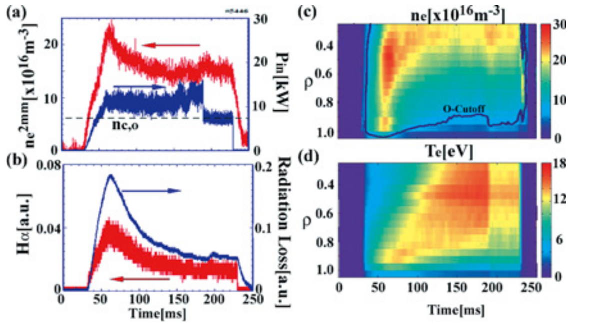

Fig. 2 (a) and (b): Time evolutions of n_e^{2mm}, P_{in}, $H\alpha$ and total radiation loss. (c) and (d): Contour plots of n_e and T_e in time and normalized radius (ρ) plane. The solid curve in (c) indicates O-mode cutoff density ($n_{c,o}$).

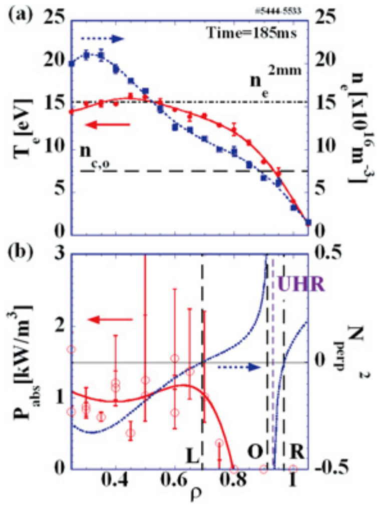

Fig. 3 (a) Radial profiles of T_e and n_e at t = 185 ms. (b) P_{abs} and squared refractive index (N_{perp}^2). Signs, such as O, R, L and UHR, respectively stand for the layers of O-mode cutoff, right-hand cutoff, the left-hand cutoff, and upper hybrid resonance.

quickly becomes peaked after t ~ 80 ms. Then, the value of n_e near the center finally becomes three times that of $n_{c,o}$. A high T_e zone propagates from the edge to the core region in time. For the shot shown in Fig. 2, the injected microwave power (P_{in}) was stepped down at t = 185 ms. The absorbed power (P_{abs}) was evaluated from the difference in the time derivative of electron energy density $3n_eT_e/2$ at each radial location on the assumption that the radiation power and the power transferred to ions smoothly evolve across the step-down. Hence, the radial profile of derived P_{abs} is shown in Fig. 3 together with those of T_e and n_e at 185 ms. As seen from Fig. 3, n_e exceeds $n_{c,o}$ within the region of ρ ~ 0.9. The microwave power is clearly absorbed inside the upper hybrid resonance (UHR) layer at ρ ~ 0.9. This suggests that "fast X-mode (FX)" - "slow X-mode (SX)" - "electron Bernstein wave (EBW)" (FX-SX-B) conversion takes place [3]. EBW, which is an electrostatic wave, can propagate into the higher density region beyond $n_{c,o}$. In this process, FX tunnels through the evanescent region between R-cutoff and UHR layers, and is converted into SX and EBW at the UHR layer. Moreover, SX is reflected almost perfectly at the L-cutoff layer, and is converted into EBW at the UHR layer. This mode conversion efficiency is expressed as

$$C = 4 \exp(-\pi\eta)(1 - \exp(-\pi\eta)) ,$$

where

$$\eta = \frac{\Omega_{ce} L_n}{c} \frac{\kappa}{\sqrt{\kappa^2 + 2(L_n/L_B)}} \left[\frac{\sqrt{1+\kappa^2} - 1}{\kappa^2 + (L_n/L_B)\sqrt{1+\kappa^2}} \right]^{\frac{1}{2}}$$

[4]. Here, κ is the ratio of electron plasma frequency for the electron cyclotron one (ω_{pe}/Ω_{ce}). L_n and L_B are the scale lengths of the electron density and magnetic field at the UHR layer. If η is less than 1, the X-mode can penetrate into the evanescent region. The maximum mode conversion efficiency, C = 1, is obtained for η = 0.22. In this experiment, the values of η and C are respectively about 0.54 and 0.6, so that appreciable mode conversion is expected. The total deposited power evaluated from Fig. 3 is about 0.5 kW across the power step-down (ΔP_{in} ~ 5 kW), and corresponds to about 10% absorption of the injected power. This low absorption rate may be due to wave power loss to the outside of the plasma through multiple reflection caused by poor wave directivity and low one-path absorption. Moreover, large density fluctuations near the edge might degrade the mode conversion rate. Under the experimental conditions shown in Fig. 1, the most plausible damping mechanism of mode-converted EBW is thought to be collisional damping near the UHR layer. However, the damping processes via the second harmonic cyclotron resonance and/or Doppler-shifted fundamental cyclotron resonance are also possible. Moreover, in cases of B_t = 0.0788 T, 0.0875 T, over-dense plasma was also generated when a fairly large amount of fuel gas was fed at higher heating power. However, the maximum of the line average electron density decreased with the increase in B_t. This reason remains uncertain.

In conclusion, over-dense plasmas have been routinely obtained with 2.45 GHz ECWs. The FX-SX-B mode conversion and absorption of the thus-generated EBW is thought to be a plausible heating scenario under the present experimental conditions. An O-X-B conversion [4-6] experiment is currently being carried out by oblique injection of the O-mode to compare it with the heating scenario based on FX-SX-B conversion. Detailed analysis of the propagation and absorption of relatively long wave-length waves (λ_0/a ~ 1, λ_0 ; wavelength of the vacuum) in a three-dimensional magnetic configuration is needed in order to clarify the damping mechanisms.

This work is supported in part by a Grant-in-Aid for Scientific Research from Japan Society for the Promotion of Science, No. 15206107.

[1] K. Toi *et al.*, 29th EPS on Plasma Physics and Controlled Fusion, Montreux, 2002, paper No. P4-061.
[2] K. Toi *et al.*, J. Plasma Fusion. Res. **6**, 516 (2004).
[3] S. Nakajima and H. Abe, Phys. Rev. A **38**, 4373 (1988).
[4] A.K. Ram *et al.*, Phys. Plasmas **7**, 4084 (2000).
[5] T. Maekawa *et al.*, J. Phys. Soc. Jpn **48**, 247 (1980).
[6] H.P. Laqua *et al.*, Phys. Rev. Lett. **78**, 3467 (1996).